Chalcogenide Letters Vol. 13, No. 9, September 2016, p. 403 - 415

EFFECTS OF Ar AND He ATMOSPHERE ON CdTe THIN FILM DEPOSITION AND CdTe SOLAR CELL PERFORMANCE

H. XU, C. LIU*, L. WU, K. LI, L. FENG, G. ZENG, S. REN, B. LI, W. LI, W. WANG, J. ZHANG
College of Materials Science and Engineering, Sichuan University, Chengdu 610064, China

Properties of polycrystalline CdTe thin film deposited under Ar and He containing atmosphere respectively as well as the performance of solar cells based on them were compared to evaluate the potential of substituting He by more economical Ar during CdTe deposition. CdTe thin films were grown in Ar-O_2 and He-O_2 mixture atmosphere by close space sublimation method. CdTe thin films of the same thickness deposited under varied atmosphere didn't show substantial property divergence, except that the deposition rate almost doubled under He containing ambience than that under Ar at the same deposition temperature. Low-temperature nucleation, sublimation and thermal convection model were introduced to interpret the large deposition rate difference under different atmosphere. Ar-atmosphere deposited CdTe solar cells had better performance than He counterpart and the optimized one showed high efficiency of 16.09%. It is highly encouraging to replace He by Ar during CdTe deposition.

(Received July 15, 2016; September 5, 2016)

Keywords: Argon, Helium, CdTe thin film deposition, Solar cell

1. Introduction

In recent years, cadmium telluride (CdTe) photovoltaic has been proven to not only have low manufacturing cost but also excellent performance [1]. The confirmed efficiency for CdTe solar cells has been boosted to 22.1% and module efficiency to 19.0%, providing a solid commercial play in competition with polycrystalline silicon-based modules [2-5].

The quality of CdTe polycrystalline thin film is a key factor to its solar cell performance. As the absorber layer, CdTe thin film has been intensively studied in the view of doping, carrier lifetime, crystallography, defect and fabrication processes [6, 7]. Inert gas, such as helium, is usually employed as deposition atmosphere to help controlling film thickness during the film deposition process via high temperature sublimation methods. Most of the CdTe thin films were deposited in He-O_2 mixture atmosphere [8]. Bas A. Korevaar and James N. Johnson's group studied the effect of oxygen during CdTe deposition for CdTe photovoltaic devices [9]. They showed that a higher amount of oxygen in the CdTe film resulted in a 10-20 mV improvement in open-circuit voltages（V_{OC}）. However, mixture gas with more than 90% volume inert gas was usually applied during the film deposition to not only eliminate CdTe source oxidation but also control film thickness. Lianghuan Feng's group persisted in a technology of close-spaced sublimation under Ar-O_2 mixture instead of He-O_2 mixture atmosphere to further decrease the fabrication cost [10]. The price of pure helium is about 10 times higher than that of argon. It shows that the cost of CdTe solar cells could be reduced by employing argon instead of helium to deposit CdTe thin film, especially in large-scale CdTe solar cell production.

For CdTe thin films prepared by close space sublimation (CSS) or vapor transport deposition (VTD), the main variables during film deposition are source and substrate

* Corresponding author: liucaicn@foxmail.com

temperature, pressure, atmosphere and so on [11-26]. In contrast with helium, argon has larger atomic radius, larger mass and lower thermal conductivity, which should have resulted in varied deposition processes and yielded CdTe thin films of different quality. However, there were few reports about the systematic study on the effect of inert gas during CdTe thin film deposition process. Thus this work focused on the different effects of Ar and He during CdTe thin film deposition process. Films were deposited in Ar-O_2 and He-O_2 mixture atmosphere with accurate experimental process controlling. The structure, morphology and optical properties of CdTe thin films were analyzed to study the effects of inert gas during CdTe thin film deposition. Solar cells were also fabricated based on them and their performance was compared.

2. Experimental

Commercial SnO_2:F-based conductive thin film on large-area glass was cut into pieces with size of 4.5 cm×6.0 cm and cleaned by ultrasonic cleaning. Cadmium sulfide (CdS) thin films were prepared on SnO_2 substrates by chemical bath deposition (CBD).

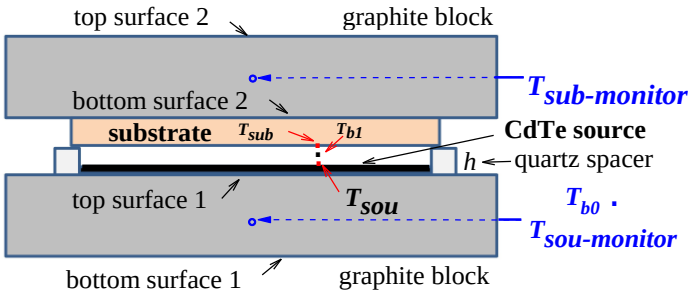

Fig. 1. Schematic illustration of CSS system for CdTe thin film deposition. The atmosphere between the surfaces of substrate and sublimation source is a mixture of inert-O_2 gas and the vapor of CdTe source. The locations of thermocouples were filled with Ar-O_2 or He-O_2.

CSS method was employed to grow CdTe thin films. A diagram of the CSS apparatus constructed for this study is presented in Fig. 1. CdTe thin films were deposited at the same temperature for 10 min to primarily calibrate the deposition rate of the films deposited under varied atmosphere. The details of the CSS system was introduced in previous work [10]. The CdTe thin films were deposited in Ar and He atmosphere with O_2 volume ratio of 8% at 3 kPa. The thickness of large-grained polycrystalline CdTe source was 1 mm. The height h of quartz spacers was 3.2 mm so that the spacing between substrate and CdTe source was 2.2 mm. The length l of quartz spacers was 60 mm. The system was filled with working atmosphere of 3 kPa when $T_{sou\text{-}monitor}$ reaches 450 ℃ without flowing to maintain a static-deposition. The conditions including source temperature ($T_{sou\text{-}monitor}$), substrate temperature ($T_{sub\text{-}monitor}$) and atmosphere were listed in Table 1.

Table 1. Primary CdTe thin film deposition rate calibration. The pinholes were observable with naked eyes under halogen tungsten lamp.

	$T_{sub\text{-}monitor}$ (℃)	$T_{sou\text{-}monitor}$ (℃)	Thickness (μm)	Deposition rate (μm/min)	Pinholes (cm^{-2})
He-O_2	530	600	8.3	0.83	0
	550	600	8.8	0.88	0
Ar-O_2	530	600	4.5	0.45	0.2
	550	600	3.7	0.37	0.6

Table 1 shows that the deposition rate of CdTe thin films deposited in He-O_2 ambient was doubled from that in Ar-O_2 atmosphere. The CdTe thin films deposited in He-O_2 showed much less pinholes than the films deposited in Ar-O_2 atmosphere. Anthony's work indicated that growth rate in He was approximately three times greater than that in Ar at large source-substrate spacing due to the smaller molecular weight and diameter of He [27]. Cruz-Campa's diffusion limited model showed that the growth rate in He was < 50% higher than that in Ar [25]. However, both Anthony and Cruz-Campa didn't conduct further analysis to find out the unknown factors of the difference of growth rates. In order to study the properties of CdTe thin films deposited under Ar-O_2 and He-O_2, CdTe thin films of similar thickness should be deposited under varied inert gas atmosphere through lowering the deposition time or source temperature of that under He, since its deposition rate is higher than that under Ar under the same conditions. It was found that the voltage controlling instead of temperature controlling is not only of better reproducibility but also helps obtaining CdTe thin films of similar thickness to study the effect of inert gas on CdTe thin film deposition by both CSS and VTD methods.

So the CdTe thin films were deposited in Ar-O_2 and He-O_2 mixed gas with oxygen volume content of 8% at the same power curve by voltage controlling (Table 2). In Table 2, the films grown under different atmosphere were deposited for the same duration time with three levels of voltage. All the films were cut into two pieces and one of them experienced varies tests and the other half was further processed to fabricate solar cells. CdTe was covered with a thin layer of $CdCl_2$ by ultrasonic method and then were annealed at 385 ℃ for 35 min in N_2-O_2 atmosphere. After heat treatment, the surface of CdTe films was etched by Br_2-methanol solution with volume ratio of 0.2% for 4 s and then gold was coated as electrode.

Table 2. Details of CdTe thin films deposition. The deposition time was 10 min. The pinholes were observable with naked eyes under halogen tungsten lamp.

Cell NO.	Voltage (V)	Temperature		Mixture atmosphere	Observation	
		$T_{sub\text{-}monitor}$ (℃)	$T_{sou\text{-}monitor}$ (℃)		Thickness (μm)	Pinholes (cm^{-2})
HeO-A	95/117	530±0	580±1	He-O_2,	4.80	0
HeO-B	100/113	540±1	580±0	3 kPa	4.02	0
HeO-C	105/110	550±4	580±1		3.60	0.1
ArO-A	95/117	540±4	605±1	Ar-O_2,	3.68	0.2
ArO-B	100/113	550±4	605±1	3 kPa	4.30	0.32
ArO-C	105/110	560±3	605±2		3.85	0.6

The surface morphology and cross-section view of the films were observed by a field emission scanning electron microscope (SEM) (Hitachi-S4300, Japan). The composition of the films on silica glass substrates was investigated by inductively coupled plasma optical emission spectrometer（ICP-OES, Spectro ACROS, Germany). The composition of the CdTe thin films on CdS was analyzed by x-ray fluorescence (XRF) (Rigaku ZSX Primus, Japan). The film thickness was measured with a step-profile system (Ambios XP-2, America). The crystal structure of the films was studied by X-ray diffractometer (XRD) (Dandong Fangyuan DX-260, China). The transmittance and reflectance of the films were characterized by an UV-Visible spectrophotometer (Perkin Elmer Lambda 950, America) with a wavelength range from 700 nm to 1100 nm. The emission spectrum of the films was characterized by photoluminescence (PL) spectroscopy (FLS980, Edinburgh Instruments Ltd, United Kingdom).

3. Results and discussion

3.1 Deposition rate of CdTe thin films

According to the results in Table 1, the CdTe thin films grown in He-O_2 atmosphere showed a deposition rate about twice of that grown in Ar-O_2. And it was observed that the system needed more power to maintain the same temperature in He-O_2. The heat and mass transfer are significantly affected by the atmosphere and possibly due to the differences between He and Ar atoms. Here, thermal convection, sublimation and mean free path models were introduced to interpret the deposition rate difference.

Conductive, natural convective and radiative heat transfer was considered in this analysis. (1) The bottom surface of the underlying graphite block which faced to bromine-tungsten lamps and received the heat mainly through thermal radiation has the highest temperature. (2) The heat was transferred to the top surface 1 of the underlying graphite block which was covered by CdTe source and the side surface which was contacted with a thermocouple through thermal conduction. (3) The heat loss might highly affected by thermal convection between the surface and inert gas.

When the power of bromine-tungsten lamps was constant, the steady-radiation and steady-conduction could be maintained in the same atmosphere. This was verified by the measured T_{sou}, T_{sub} and thickness of CdTe films. Precise power curve of bromine-tungsten control leads to the same temperature curve and expected thickness of CdTe thin films. However, the temperature curve might change if the atmosphere was different even though at the same heating power. This is due to the different thermal convection transfers in different atmosphere. The thermal convection was described by newton's cooling equation [28] as following:

$$q'' = h_1(T_s - T_b) \quad (1)$$

where q'' is the heat flux, h_1 is the convective transfer coefficient, T_s is the temperature on solid surface and T_b is environmental temperature.

The convective transfer coefficient is influenced by several factors including location, pressure, flow velocity and physical properties of gas. Here, the CdTe thin films were deposited in Ar-O_2 and He-O_2 at the same pressure and remained the power curve same. The convective transfer coefficient was mainly influenced by the thermal conductivity of Ar-O_2, He-O_2 and the vapor from CdTe source. The value of h_1 near the side surface of graphite block was mainly influenced by the thermal conductivity of inert gas. The value of h_1 near the top surface of graphite block was not only influenced by inert gas but also by the

vapor of CdTe source. When the temperature was lower than 550 ℃ which represents the nucleation stage of CdTe thin film growth, the vapor pressure of CdTe source was much lower than the partial pressure of inert gas and can be neglected in Equation 1. As the deposition temperature increases, the partial pressure of Cd and Te_2 from CdTe source increases rapidly and can no longer be neglected in Equation 1, especially for the CSS system with height/length (*h*/*l*) ratio of quartz spacer lower than 5%. The nucleation of CdTe thin film growth starts when T_{sub} and T_{sou} raise to 400 ℃ and 450 ℃ respectively. And the deposition process changes to high growth rate stage instead of nucleation stage as the T_{sou} raises to temperature higher than 550 ℃. As we know that the thermal conductivity of He is ten times higher than that of Ar. The T_{sub} is influenced by thermal conductivity of inert gas through natural thermal convection. Higher thermal conductivity leads to lower T_{sub} in He-O_2 during the nucleation stage of CdTe film growth. The mean free path λ of Cd atoms and Te2 molecules is influenced by temperature and pressure. The average free path is lower than the distance between CdTe source and substrate (λ < h) when Tsou < 550 ℃. The nucleation of CdTe thin film growth may well be described by clausius mean free path model when T_{sou} is lower than 550 ℃. The Clausius mean free path model of gas molecules as formula [29]:

$$\bar{\lambda} = \frac{kT}{\sqrt{2}\pi d^2 p} \tag{2}$$

where $\bar{\lambda}$ is the average mean free path of Cd, Te and CdTe molecular, d is the effective molecular diameter and p is pressure. According to Equation 2, the mean free path is dominantly influenced by the effective molecular diameter of mixed gas atmosphere at the same temperature. It was reported that the value of *d* for He is smaller than that of Ar ($d_{He,\infty}$= 0.222 nm, $d_{Ar,\infty}$=0.299 nm). So the average mean free path in He-O_2 is larger than that in Ar-O_2. Larger average mean free path leads to higher density of nucleation in He-O_2 than that in Ar-O_2.

As T_{sou} increases from 550 ℃ to 600 ℃, deposition of CdTe thin films changes to sublimation model at pressure lower than 40 Torr (~ 5.3 kPa) [25]. From the sublimation model, the average deposition rate is between 0.5-0.75 μm/min in Ar. This is very close to the experiment data 0.37-0.45 μm/min in Ar-O_2 in Table 1. However, CdTe deposition rate was 0.83-0.88 μm/min in He-O_2, which was twice of that in Ar-O_2. It does not match the sublimation model well. This is because of the difference between the monitored temperature and real temperature of the substrate and CdTe source in different atmosphere. The atmosphere near the thermocouple was only inert gas so that the measured $T_{sou\text{-}monitor}$ and $T_{sub\text{-}monitor}$ were greatly influenced by inert gas through thermal convection. Meanwhile, the T_{sou} and T_{sub} were greatly influenced by vapor from CdTe source at temperature from 550 ℃ - 600 ℃. According to the thermal convection model, the measured $T_{sou\text{-}monitor}$ and $T_{sub\text{-}monitor}$ in He was much lower than that in Ar even though the T_{sou} and T_{sub} in different atmosphere was nearly the same when $T_{sou\text{-}monitor}$ and $T_{sub\text{-}monitor}$ was higher than 550 ℃. And the experimental data shows that the measured temperature $T_{sou\text{-}monitor}$ and $T_{sub\text{-}monitor}$ in He-O_2 was about 25 ℃ lower than that in Ar-O_2 during the high rate deposition stage. The mean free path of Cd and Te in helium is relatively larger than that in argon, which should lead to higher deposition rate in He-O_2 during the nucleation stage of CdTe thin film growth.

In a word, T_{sub} and average mean free path are influenced by inert gas during the nucleation stage of CdTe film deposition process, which could be analyzed by thermal convection and mean free path theory. The dependence relationship between monitored and true source and substrate temperature was influenced by both inert gas and CdTe vapor. CdTe thin film deposition matches thermal convection and mean free path model when T_{sou} is lower than 550 ℃. And it matches sublimation model when T_{sou} increases from 550 ℃ to 600 ℃. Table 2 shows that nearly the same film thickness could be obtained when the films were deposited at the same voltage (power) but at different $T_{sou\text{-}monitor}$ and $T_{sub\text{-}monitor}$ in Ar-O_2 and He-O_2. CdTe thin films with less pinhole were produced in He-O_2 due to high density and low T_{sub} of nucleation.

3.2 Crystal structure

All the CdTe thin films were of face-centered cubic structure and preferred to the orientation to (111) direction. The films deposited in Ar-O_2 and He-O_2 ambience also both showed minimal orientation along (220), (311), (331) and (400) directions. CdTe thin films deposited in He-O_2 had relatively stronger intensity in (220) and (311) compared to the films grown in Ar-O_2 atmosphere (Fig. 2).

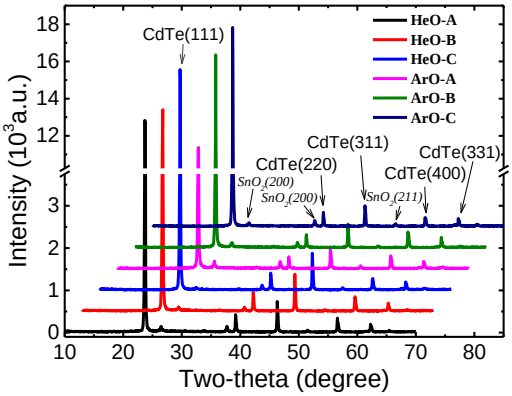

Fig. 2. XRD patterns of as-deposited CdTe thin films.

Meanwhile, samples of ArO-B and ArO-C had the highest texture coefficient at plane (111), which means better single orientation crystallinity and quality and is beneficial to eliminating grain boundaries and the carrier recombination at there. It is well known that better single orientation crystallinity, higher grain quality and less grain boundaries are beneficial to improve V_{oc} and *FF* of CdTe solar cells. This indicates that CdTe thin films deposited in Ar-O_2 atmosphere are more potential to yield higher V_{oc} and *FF* of CdTe solar cells than that in He-O_2.

Table 3. The texture factor extracted from XRD patterns to describe the preferred orientation.

	Texture coefficients				
	(111)	(220)	(311)	(400)	(331)
HeO-A	2.75	0.15	**0.52**	1.18	0.40
HeO-B	2.69	0.15	**0.60**	1.17	0.38
HeO-C	3.00	0.14	**0.59**	0.91	0.37
ArO-A	2.67	0.13	**0.40**	1.36	0.44
ArO-B	2.84	0.10	**0.37**	1.22	0.47
ArO-C	3.37	0.12	**0.36**	0.76	0.40

3.3 Film morphology

The average grain size range between 2-3 micrometers was derived from the surface morphology of the CdTe thin films deposited in Ar-O_2 and He-O_2 atmosphere (Fig. 3).

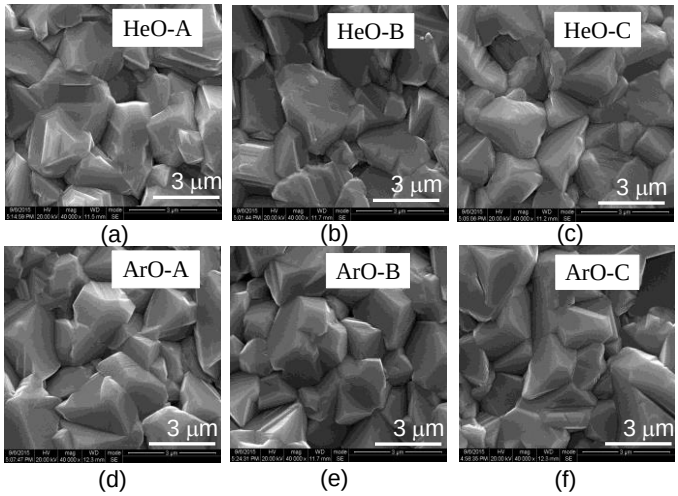

Fig. 3. SEM graphs of the samples deposited in Ar-O_2 and He-O_2 mixture atmosphere.

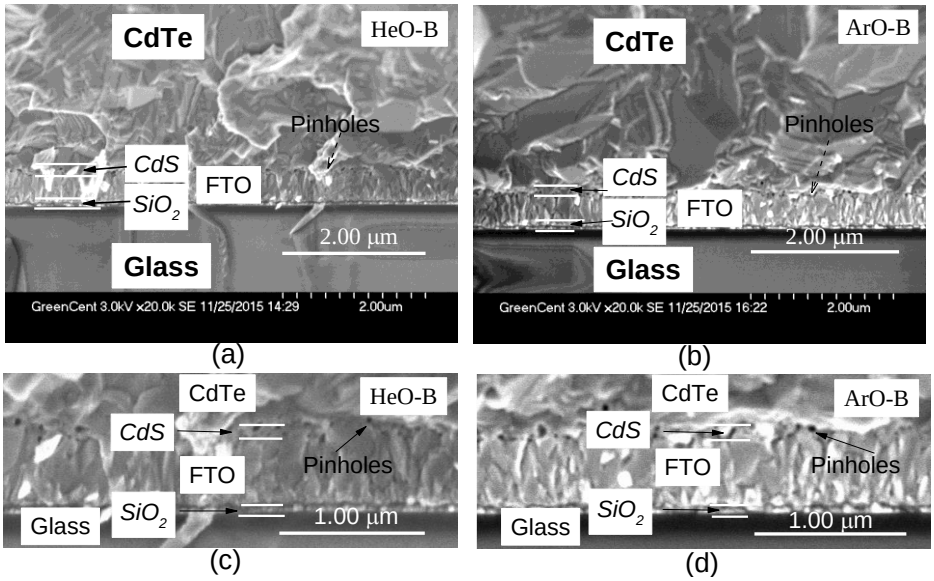

Fig. 4. Cross section SEM graphs of the samples deposited in Ar-O_2 and He-O_2 atmosphere.

In Fig. 3, the surface morphology shows that the films deposited in He-O_2 mixture atmosphere achieved similar grain size to that of the films deposited in Ar-O_2 mixture atmosphere. The cross-section micrographs showed that the film grown in He-O_2 was of smaller pinholes at the interface of CdS/CdTe. Nearly the same film thickness about 4 μm of ArO-B and HeO-B was also observed in the cross-section graphs (images not shown here), even though the measured temperature of CdTe source was different (as listed in Table 2). The deposition rate and grain size of CdTe thin film are mainly influenced by $T_{sou} > 550$ ℃ and T_{sub}. The size and number of pinholes at the interface of CdS/CdTe are influenced by nucleation stage of CdTe thin film deposition process which is mainly influenced by T_{sub} and mean free path of atoms from CdTe source. These results indicated that He-O_2 atmosphere might resulted in higher density nucleation than that in Ar-O_2 during CdTe thin film deposition process. The system was at the same T_{sou} and T_{sub} in Ar-O_2 and He-O_2 even though

the value of $T_{sou\text{-}monitor}$ and $T_{sub\text{-}monitor}$ was higher in Ar-O_2. The results are consistent with the previous thermal convection, mean free path and sublimation models.

3.4 Composition and compactness

The atomic Cd/Te ratio of the films on silica glass substrates was about 1.06 measured by ICP-OES method, which means that the CdTe films were Cd-rich. X-ray fluorescence method was employed to probe the composition of the CdTe thin films grown on CdS substrates. K_α and K_β transition radiation from the irradiation area with 1 cm diameter were chosen as the characteristic spectra for cadmium and tellurium. For the CdTe thin films, lower Cd/Te ratio means more V_{Cd}. The average Cd/Te ratio for CdTe thin films grown in He-O_2 was 1.183 while that in Ar-O_2 atmosphere showed a little more Cd-rich with Cd/Te ratio about 1.188, as listed in Table 4. It was probable that the CdTe thin films deposited in He-O_2 have more V_{Te} than that in Ar-O_2. The effect of V_{Te} on CdTe solar cells is complicated. The compactness of the films was defined as following:

$$C_o = D_m / D_0 \tag{3}$$

where C_o is the compactness factor, D_m is the mass-thickness calculated out by XRF system and D_0 is the thickness investigated by a step-profile system. Larger D_m means higher density of the measured film with the same profile-thickness. From a theoretical point of view, the films with higher density usually have less point defect, and pinholes. It is reasonable that higher compactness factor means higher thin film crystal quality. Table 4 shows that CdTe thin films deposited in Ar-O_2 were of higher compactness factor than that in He-O_2. However, the compactness factor decreased rapidly as T_{sou} and T_{sub} increased due to the emergence of pinholes in Ar-O_2 atmosphere. These indicate that the CdTe thin films deposited in Ar-O_2 are with less point defect but larger pinholes than that in He-O_2. The pinholes formed because of lower density of nucleation in Ar-O_2 than that in He-O_2. Higher crystal quality of CdTe thin films usually leads to higher V_{oc} and FF for CdTe solar cells. However, the increases of pinhole-size can leads to short-circuit between window layer and back contact layer in CdTe solar cells. It was found that the He-O_2 atmosphere which leads to less pinhole of CdTe thin films caused by high density nucleation is beneficial to large-area CdTe solar cells manufacture.

Table 4 The compactness and composition of CdTe thin films.

	Compactness (%)		Cd/Te ratio	
	He-O_2	Ar-O_2	He-O_2	Ar-O_2
A	69.4	75.8	1.176	1.185
B	70.0	71.2	1.181	1.185
C	69.7	69.8	1.192	1.193

3.5 Optical properties

The optical band gaps were calculated from the following expression by assuming a direct transition between valance and conduction bands:

$$(\alpha h\nu)^2 = D(h\nu - Eg) \tag{4}$$

where D is a constant, h is the Plank's constant and α is the optical absorption coefficient.
The energy band gap can be estimated by extrapolating the straight-line portion of the spectrum to a zero absorption coefficient value.The band gap for all the films is 1.50 eV. Fig.

5 shows the absorbance spectra of CdTe thin films. The Lambert-Beer theory which is usually used for solution concentration analysis can be described as formula:

$$A = \varepsilon bc \tag{5}$$

where ε is molar absorptivity, b is the volume and c is the concentration of solution.

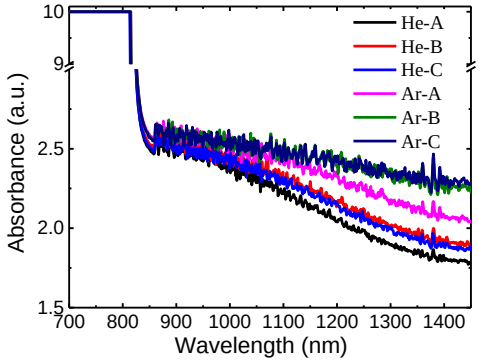

Fig. 5. The absorbance spectra of CdTe thin films.

The Lambert-Beer theory seems hard to be used for solid analysis because of the enough higher concentration to absorb the incident light. So the absorbance at wavelength less than 800 nm is 10 which means fully absorbed. When the wavelength increases to 1400 nm, the energy of incident light become lower and difficult to be absorbed by CdTe film, the suitability of Lambert-Beer theory increases as well. And higher absorbance means higher density of CdTe film. From Fig. 5, it can be seen that the films deposited in Ar-O_2 are with relatively higher compactness which corresponds to the XRF results in Table 3.

Fig. 6 shows the emission spectra with energy ranged from 1.0 eV to 1.8 eV of the CdTe thin films grown in different atmosphere. As the general case in most semiconductors, defects in p-CdTe also could be divided into three main types: shallow, deep and mid-gap [30]. Three kinds of transition were observed in the as-deposited CdTe thin films. The transition peaks at 1.42-1.44 eV which possibly represent donor-acceptor pair transition are very close to the transition from valence band to conduction band 1.50 eV.

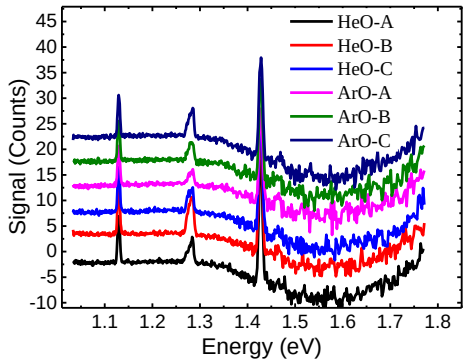

Fig. 6. PL emission spectra of CdTe films measured at 300 K, with excitation laser beam wavelength of 655 nm

The ionization energy within 60-80 meV above the valence band maximum is corresponding to shallow defects. Impurities from group V, such as nitrogen and phosphorus are also known to yield shallow extrinsic p-type defects in CdTe [30, 31]. The emission with transition energy ranged from 1.26 to 1.29 eV was observed in CdTe thin films deposited in varied atmosphere (Fig. 6). This kind of emission shifted with the excitation wavelength. The emission varied from 934-1018 nm when the excitation wavelength ranged from 630-690 nm. The intensity of such emission changed with the excitation wavelength as well. The highest emission was at 970 nm at excitation wavelength of 660 nm. Such a behavior called red-edge-effect (REE) was observed for nanoparticles and ionic liquids containing the dipolar solute [32]. It was considered that more tests, such as Raman measurement, need to be conducted to determine that. Another kind of deeper defect with transition energy ranged in 1.12 eV-1.13 eV was also detected. There is little reported data for the defect with ionization energy within 370-380 meV. Further experimental and theoretical studies need to be conducted.

3.6 Device performance

In order to avoid the fluctuation which may be caused by back contact layer, Au electrode was evaporated onto CdTe directly during device fabrication. In Fig. 7 (a), the results show that CdTe solar cells were fabricated at optimized temperature range and relatively higher T_{sou} and T_{sub} led to poor CdTe solar cell performance. The solar cells manufactured in Ar-O_2 showed sharper performance degradation than that prepared in He-O_2 atmosphere as the source and substrate temperature was elevated, which possibly due to the increase of pinhole size. CdTe solar cell with the best efficiency of 11.19% was prepared in Ar-O_2. The quantum efficiency (QE) of the CdTe solar cells is illustrated in Fig. 7 (b). Fig. 7 (b) shows that QE curves of the cells with CdTe thin films deposited in He-O_2 and Ar-O_2 were similar. The substrate in He-O_2 was with lower temperature until the nucleation stage transformed to high rate deposition stage. Substrate temperature is critical for desublimation when T_{sub} > 450 ℃ during the CdTe thin film deposition process. Lower T_{sub} decreases the desublimation of Cd, Te and CdTe molecules and probably leads to high density of nucleation in He-O_2. This is important for the stability of CdS/CdTe interface at higher temperature. And nucleation at lower temperature would weaken the interfacial diffusion which is not conducive to higher device performance. High density of nucleation can increase grain boundary at CdS/CdTe interface and possibly decreases V_{oc} of CdTe solar cells. High efficiency CdTe solar cells prepared in He-O_2 atmosphere were reported by other groups [9, 33]. We optimized the cell structure and prepared CdTe solar cells in Ar-O_2 and high efficiency over 16% was obtained (as shown in Fig. 8 (a) and Fig. 8 (b)).

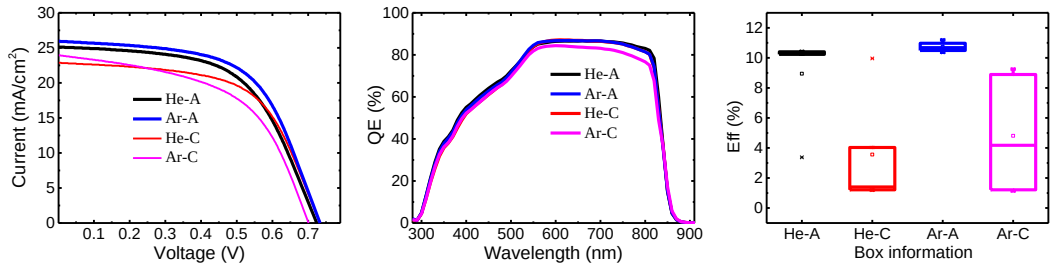

Fig. 7. The light I-V and QE curve of the best CdTe solar cell fabricated at various temperature in different atmosphere.

Table 5. Light I-V parameters of the best CdTe solar cells.
The area of each CdTe solar cells is 0.188 cm^2.

	Eff (%)	FF (%)	Jsc (mA/cm^2)	Voc (mV)	Rsh ($\Omega*cm^2$)	Rs ($\Omega*cm^2$)
He-A	10.43	57.3	25.1	724.0	446.2	7.9
He-C	9.96	59.4	22.9	733.3	405.3	7.9
Ar-A	11.19	58.8	25.9	733.3	364.0	7.4
Ar-C	8.89	52.9	24.0	701.3	152.6	7.4

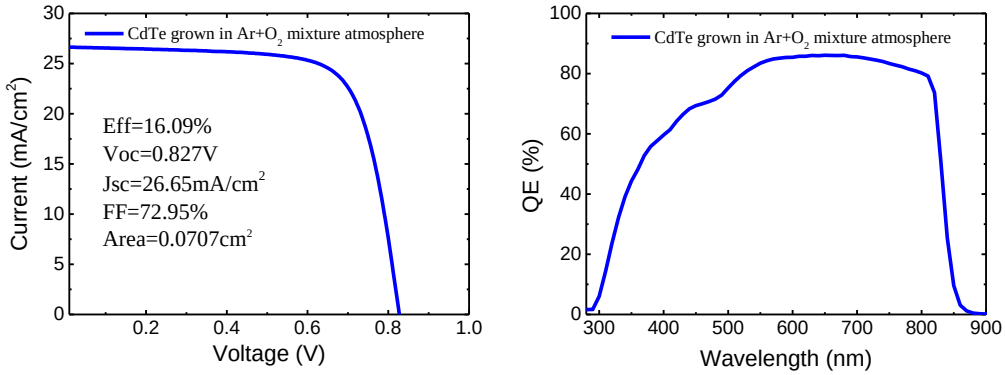

(a) (b)

Fig. 8. Light J-V and QE curve of the optimized CdTe solar cell with CdTe thin film grown in Ar-O_2 atmosphere. The light J-V curve was measured under global AM 1.5 spectrum (1000 W/m^2) at 25 ℃ of CdTe solar cell. The structure is glass/FTO/SnO_2/sputtered-CdS:In/CdTe/ZnTe:Cu/Au.

4. Conclusion

Deposition processes, film properties and device performance of CdTe prepared under Ar-O_2 and He-O_2 atmosphere was compared systematically. Different thermal conductivity and atom radius between He and Ar resulted in varied thermal convection and mean free path effects on the nucleation stage of CdTe film deposition. The high rate deposition stage of CdTe thin film growth process is sublimation model. The relationship between true and monitored source and substrate temperature was highly affected by thermal conductivity of inert gas. Voltage controlling method was introduced for the film's high rate deposition stage to achieve equal T_{sou} and T_{sub} in He-O_2 and Ar-O_2. Ar-O_2 atmosphere led to higher crystal quality, higher compactness and better optical properties of CdTe thin films than that in He-O_2. Cells with higher performance were fabricated from CdTe films prepared in Ar-O_2 atmosphere. CdTe solar cells with efficiency higher than 16% were obtained in Ar-O_2 atmosphere as well. In this study, Ar showed the potential to yield competitive or even better device performance than He, and its possible to replace He in mass production as its lower cost.

Acknowledgements

This work is financially supported by the National High Technology Research and Development Program of China No. 2015AA050610. And we would like to thank the Analytical and Testing Center of Sichuan University for ICP-OES measurement.

Reference

[1] O. Zelaya, F. Sánchez-Sinencio, J. G. Mendoza-Alvarez, M. H. Farías, L. Cota-Araiza, G. Hirata-Flores, J. Appl. Phys. **63**, 410 (1988).
[2] M. A. Green, K. Emery, Y. Hishikawa, W. Warta, E. D. Dunlop, Prog. Photovolt.: Res. Appl. **23,** 1 (2015).
[3] A. Teyou Ngoupo, S. Ouédraogo, F. Zougmoré, J. M. B. Ndjaka, Int. J. Photoenergy **2015**, 1 (2015).
[4] Martin A. Green, Keith Emery, Yoshihiro Hishikawa, Wilhelm Warta, Ewan D. Dunlop, Prog. Photovolt.: Res. Appl. **23**, 805 (2015).
[5] http://investor.firstsolar.com/releasedetail.cfm?ReleaseID=956479.
[6] Zimeng Cheng, Alan E. Delahoy, Zhaoqian Su, Ken K. Chin, Thin Solid Films **558,** 391 (2014).
[7] R. Ramírez-Bon, F. J. Espinoza-Beltrán, H. Arizpe-Chávez, O. Zelaya-Angel, F. Sánchez-Sinencio, J. Appl. Phys. **79**, 7682 (1996).
[8] D. S. Albin, Y. Yan, M. M. Al-Jassim, Prog. Photovolt.: Res. Appl. **10**, 309 (2002).
[9] Bas A. Korevaar, James R. Cournoyer, Oleg Sulima, Aharon Yakimov, James N. Johnson, Prog. Photovolt.: Res. Appl. **22,** 1040 (2014) .
[10] L. Feng, J. Zhang, B. Li, W. Cai, Y. Cai, L. Wu, Thin Solid Films **491,** 104 (2005).
[11] T. M. Razykov, S. Zh Karazhanov, A. Yu Leiderman, N. F. Khusainova, K. Kouchkarov, Sol. Energy Mater. Sol. Cells **90,** 2255 (2006).
[12] L. A. Kosyachenko, E. V. Grushko, V. V. Motushchuk, Sol. Energy Mater. Sol. Cells **90,** 2201 (2006).
[13] P. Horodyská, P. Němec, T. Novotný, F. Trojánek, P. Malý, J. Appl. Phys.**116,** 053913 (2014).
[14] J. T-Thienprasert, T. Watcharatharapong, I. Fongkaew, M. H. Du, D. J. Singh, S. Limpijumnong, J. Appl. Phys. **115,** 203511 (2014).
[15] Marco Nardone, J. Appl. Phys. **115,** 234502 (2014).
[16] F . A. Ponce R. Sinclair , T. Yamashita , D. J. Smith , R. A. Camps , L. A. Freeman, S. J. Erasmus , W. C. Nixon , K. C. A. Smith , C. J. D. Catto, Nature **298,** 5 (1982).
[17] P. E. Batson K. A. Mkhoyan, J. Cha, W. J. Schaff, J. Silcox, Sci Bull. **312,** 1 (2006).
[18] Y. Y. Proskuryakov, K. Durose, J. D. Major, M. K. Al Turkestani, V. Barrioz, S. J. C. Irvine, Sol. Energy Mater. Sol. Cells **93,** 1572 (2009).
[19] J. D. Major, Y. Y. Proskuryakov, K. Durose, Prog. Photovolt.: Res. Appl. **21**, 436 (2013).
[20] A. Kanevce, D. H. Levi, D. Kuciauskas, Prog. Photovolt.: Res. Appl. **22,** 1138 (2014).
[21] H. N. Jayatirtha, D. O. Henderson, A. Burger, M. P. Volz, Appl. Phys. Lett. **62,** 573 (1993).
[22] C. W. Warren, J. Li, C. A. Wolden, D. M. Meysing, T. M. Barnes, D. Westley Miller, Appl. Phys. Lett. **106**, 203903 (2015).
[23] J. P. Enríquez, E. Gómez Barojas, R. S. González, U. Pal, Sol. Energy Mater. Sol. Cells. **91,** 1392 (2007) .
[24] M. Terheggen, H. Heinrich, G. Kostorz, A. Romeo, D. Baetzner, A. N. Tiwari, Thin Solid Films **431-432,** 262 (2003).
[25] J. L. Cruz-Campa, D. Zubia, Sol. Energy Mater. Sol. Cells **93,** 15 (2009).
[26] M. E. Hernández-Torres, R. Silva-González, G. Casarrubias-Segura, J. M. Gracia-Jiménez, Sol. Energy Mater. Sol. Cells **90**, 2241 (2006).
[27] T. C. Anthony, J. Vac. Sci. Technol. A, **2**, 1296 (1984).

[28] M. I. Davidzo, Int. J. Heat Mass Tran. **55,** 5397 (2012).
[29] Z. Cheng G. Liu, G. E. Georgiou , K. K. Chin. Proceedings of the 42th IEEE photovoltaic specialists conference 2015.
[30] T. A. Gessert, S. H. Wei, J. Ma, D. S. Albin, R. G. Dhere, J. N. Duenow, et al., Sol. Energy Mater. Sol. Cells **119,** 149 (2013).
[31] T. Baron, K. Saminadayar, N. Magnea, J. Appl. Phys. **83**. 1354 (1998).
[32] B. Murali, S. B. Krupanidhi, J. Appl. Phys. **114,** 144312 (2013).
[33] X. Wu, Solar Energy **77**, 803 (2004).